



OPEN AI-based prediction and detection of early-onset of digital dermatitis in dairy cows using infrared thermography

Marcelo Feighelstein¹, Amir Mishael², Tamir Malka², Jennifer Magana⁴, Dinu Gavojdian³✉, Anna Zamansky¹✉ & Amber Adams-Progar⁴

Digital dermatitis (DD) is a common foot disease that can cause lameness, decreased milk production and fertility decline in cows. The prediction and early detection of DD can positively impact animal welfare and profitability of the dairy industry. This study applies deep learning-based computer vision techniques for early onset detection and prediction of DD using infrared thermography (IRT) data. We investigated the role of various inputs for these tasks, including thermal images of cow feet, statistical color features extracted from IRT images, and manually registered temperature values. Our models achieved performances of above 81% accuracy on DD detection on 'day 0' (first appearance of clinical signs), and above 70% accuracy prediction of DD two days prior to the first appearance of clinical signs. Moreover, current findings indicate that the use of IRT images in conjunction with AI based predictors show real potential for developing future real-time automated tools to monitoring DD in dairy cows.

Digital dermatitis (DD) is a serious infectious disease affecting the feet of dairy cattle, which has detrimental effects on their production, economic value, and the overall animal wellbeing^{1,2}. DD has been linked to decreased milk yields, severe lameness and fertility declines, and is regarded as one of the major welfare issues in the dairy industry³. Although much research has been done on the lameness of cattle, such as identifying associated risks⁴ or selection for health and fitness⁵, the prevalence of lameness remains high due to the lack of reliable early onset diagnosis and prognosis tools.

Recent developments in farming precision technologies (PLFs) have advanced machine learning approaches for accelerometer activity analysis and a timely diagnosis of various cattle diseases^{6–10}. Most of the works in this domain employed sensor-based behavior data. Currently, a wide range of commercially-validated systems collecting such data are available¹¹, which can monitor behavioral patterns such as feeding, ruminating, activity, and lying. Alterations in some of these behavioral patterns have been directly linked to DD in dairy cattle, with ill animals spending more time lying down than their healthy counterparts, while devoting less time to feeding and rumination^{12,13}. Magana et al.¹⁴ was the first to present a machine learning approach based on behavioral data collected by accelerometers, for early-onset detection and prediction of DD in cows, reaching 79% and 64% (two days prior to the appearance of symptoms) accuracy respectively.

Several works explored the use of thermal images (IRT) in the context of DD to-date. For instance, Harris-Bridge et al.¹⁵ used statistical descriptors and compared the use of IRT imaging at the heel and coronary band levels, revealing significant differences between healthy and DD affected feet. Anagnostopoulos et al.¹⁶ explored how IRT interdigital skin temperature correlates with various stages of DD lesions and developed logistic regression models to detect active DD lesions. Vanhoudt et al.³ further examined the use of IRT as a diagnostic method for detecting painful lesions associated with DD in dairy cattle, under commercial farm environments. Their study involved the evaluation of hind feet for active lesions, findings indicating that higher maximum IRT temperatures from unwashed feet were significantly linked to the presence of DD lesions. Authors found that these associations persisted even after the feet were washed; however, the reliability of IRT and DD association decreased, with the study concluding that the use of IRT could serve for automated monitoring of foot health in order to identify animals at risk of developing DD. Computer vision-based approaches for automated detection and prediction DD remains largely underexplored. Cernek et al.¹⁷ developed a computer vision-based model for DD detection using a large database of videos screenshots images from commercial farm settings, the model

¹University of Haifa, Haifa, Israel. ²Technion,, Haifa, Israel. ³Research and Development Institute for Bovine, Balotesti, Romania. ⁴Washington State University, Pullman, WA, USA. ✉email: gavojdian_dinu@animalsci-tm.ro; annazam@is.haifa.ac.il

reaching an accuracy of 88% in detecting active DD lesions. Aravamuthan et al.¹⁸ studied lightweight YOLOv4 models deployed on edge devices for real time detection of DD. However, timely prediction of DD prior to the appearance of clear signs is extremely challenging. To the best of our knowledge, this current study is the first to investigate computer vision techniques applied to thermal feet images, for both detection and early onset prediction of DD in dairy cattle. In addition to thermal images, we included other sources of information, including statistical color features extracted from these images, and manually registered temperature values. We thus developed and tested deep learning-based models for early onset detection and prediction of DD in lactating dairy cattle.

Methods

Data collection

Ethics and animal handling: All procedures used in the current study were approved by the Washington State University Institutional Animal Care and Use Committee (IACUC), approval code ASAF#6770 issued on 15 of April, 2020. All methods were carried out in accordance with relevant guidelines and regulations. Data collection was based on a non-invasive observational trial, with no additional pain or stress being induced to the animals, following strictly naturally occurring bovine digital dermatitis. Furthermore, best practices for animal handling, prevention, diagnostic and treatment of digital dermatitis were applied on-farm, with cows being continuously monitored by a trained veterinarian. All methods are reported in accordance with ARRIVE guidelines.

The study was carried out for 60 consecutive days at the Washington State University Knott Dairy Center (KDC) in Pullman, WA, U.S. The experimental farm houses 180 Holstein cows, with lactating animals being housed in a free-stall barn with individual stalls, using composted manure as bedding. Cows were milked twice daily, using a 6 by 6 'herring-bone' milking parlor, in which animals had ad libitum access to two water troughs, were fed a total mixed ration and fitted with CowManager® individual accelerometers. The KDC experimental farm practices indoor housing year-around for lactating cows, with movement alleys and the outside paddock having concrete flooring.

Cattle were enrolled into the study if they were clinically healthy at the start of the data-collection, while having no lesions for at least seven recorded days prior to the first observation of an active DD lesion, and had over two consecutive days of DD lesion observed. During the trial, a total of 17 cows (ranging from 1st to 5th parities) developed DD and met the criteria for enrolment. Each cow that developed a DD episode was then matched with a healthy counterpart (control group), animals with the same parity, reproduction status (open/pregnant), and lactation period (early/mid/late). Lactation periods were classified as early (first 100 days in milk (DIM)), mid (between 101 and 199 DIM), or late (>199 DIM).

As a DD prevention method, an acidified copper-, sulfate- and zinc footbath solution was placed at the exit from the milking parlor, with the footbath solution being replaced twice a week. The human-observer for this study was previously trained by a hoof specialist to evaluate digital dermatitis (DD) lesions. All hoofs were visually assessed during morning milkings inside the milking parlor, looking exclusively at the hind feet. When DD lesions were observed, the observer then categorized them as active or digressing, with lesion size being evaluated and categorized based on diameter as either small (under 0.6 cm), medium (0.6–3.8 cm), or large (over 3.8 cm). The same observer recorded the DD status and lesion size daily during the trial, in order to avoid inter-observer biases. As a result, the final dataset included 17 cows that developed DD and 21 healthy counterparts, with IRT and sensor data being collected at least 7 days prior to the DD diagnosis.

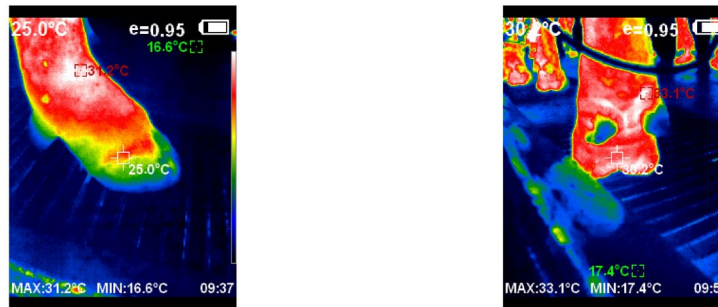
The thermographic images were taken using an IRT gun (model HTI HT-19, XT Instrument Co., Dongguan, China) and further used to investigate computer vision techniques in this context, in order to assess hoof temperature changes. Images were taken once the hind feet were sprayed with water and the individual cows were locked in the milking parlor, in order to minimize environmental factors. Using the IRT gun, the observer captured all images at approximately the same distance (35 cm), perpendicular from the hoof, while ensuring that the coronary band was clearly visible. IRT images were taken of the rear feet of all 180 dairy cows daily, as the development of DD was not controlled and could develop spontaneously. In each captured image per foot, the areas measured using the IRT gun were the coronary band and the heel, taking one picture per region/foot/day.

Dataset

The original dataset comprised of 569 IRT images, each with dimensions of 240 pixels x 320 pixels, displaying the feet of 17 individual cows captured during the experimental trial. These images were obtained from two different perspectives: one focusing on the heel and the other on the coronary band (CB). Each image has been categorized as either 'healthy' or 'DD' based on the clinical examination conducted at the time of image capture.

The distribution of images per cow, their health status, indication of left or right feet, and the specific angle captured (CB or Heel) are presented in the supplement.

The number of IRT images varied for each individual cow, ranging from 18 to 46, with an average of 33 IRT images per cow. In total, 463 images were classified as 'healthy' (81%), while 106 were labelled as 'DD'. The dataset was comprised of 312 IRT images of coronary bands and 257 IRT images of heels, maintaining the ratio between healthy-labeled and DD-labeled images for each individual foot. All cows included in the final dataset exhibited signs of DD, ensuring impartiality in the classifier to avoid potential biases that may arise if one single cow had only healthy-labeled images. This uniformity prevented the classifier from learning specific features of individual cows, and instead focused on identifying the DD presence in the images analyzed. The IRT images were organized and labeled with a day stamp relative to the initial diagnosis of the DD episode (Day 0), spanning from 7 days prior to the diagnosis, up to 7 days post DD-diagnosis. The dataset was structured based on cow ID, foot region (heel or CB), healthy or DD class (label), and the day stamp. It is important to note that an animal could be categorized as 'DD' or 'healthy' on any day following Day 0, while it was consistently labeled as 'healthy' before Day 0.



(1) Left Feet, Coronary Band, 1 day after DD detection (2) Right Feet, Heel, 2 days after DD detection

Figure 1. Raw image examples.

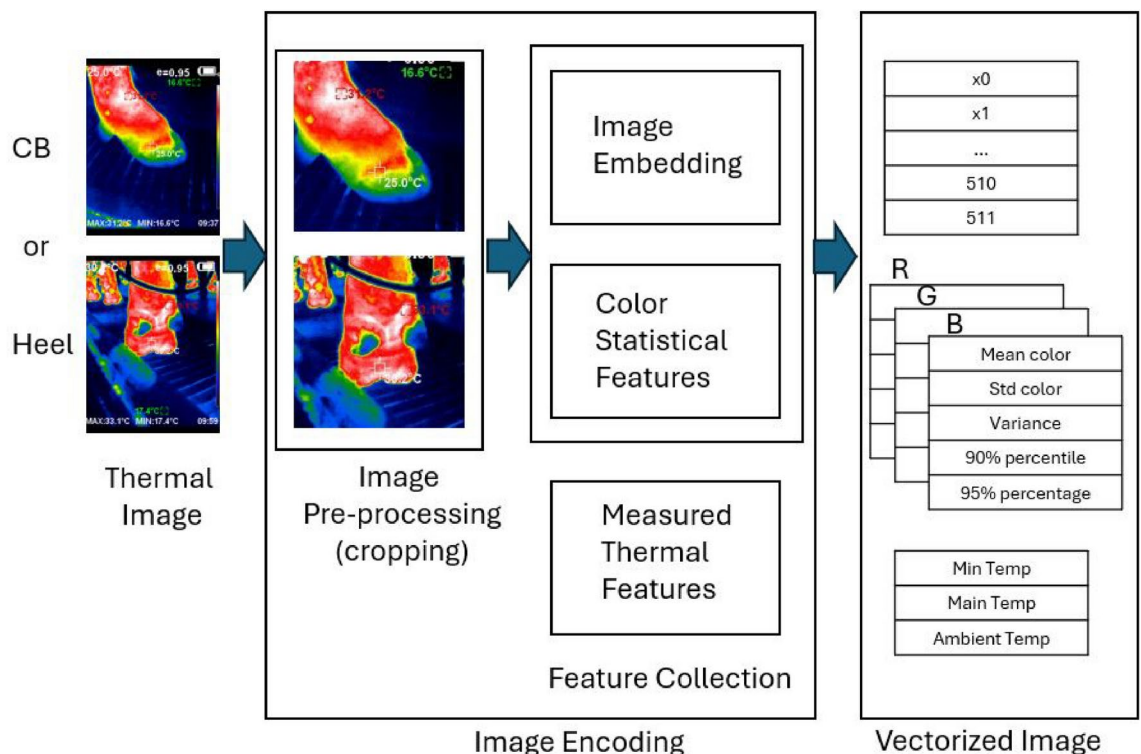


Figure 2. Image encoding block diagram.

The images were organized and labeled with a day stamp relative to the initial diagnosis of DD (Day 0), spanning from 7 days prior to the diagnosis to 7 days post-diagnosis. The dataset was structured based on cow ID, leg parts, class (label), and day stamp. It's important to note that an animal could be categorized as Sick or Healthy on any day following Day 0, while it was consistently labeled as Healthy before Day 0.

Figure 1 shows IRT image samples taken from cow identified as 179: (1) showing the CB from left feet taken 1 day after DD detection and (2) showing the Heel angle for right feet taken 2 days after DD detection.

AI pipelines overview

In this study, we introduced two distinct pipelines utilizing thermal images of cows' feet: the first pipeline focused on identifying DD based on a single image, while the second pipeline predicted DD episodes based on images of the same animal captured from the same angle (CB or heel) on two consecutive days. Both pipelines employed the same encoding process, which consisted of image embedding with the additional integration of statistical and thermal features, as shown on Fig. 2. We explain these steps in further details below.

Image cropping

This step was performed to eliminate redundant information (noise) from the images; therefore we applied cropping around the cow foot. Since all of the images were taken from a relatively constant angle, the cropping

region was cropped at [30:230, 20:220] (height, width). The resulting cropped image dimensions were 200 * 200 * 3, containing mostly the foot.

Feature extraction

Given the influence of Digital Dermatitis (DD) on the thermal profile of a cow's leg¹⁶, our hypothesis proposed that significant features can be extracted from thermal images to detect the onset of the condition. The process of image encoding maps the input data into a lower-dimensional representation while preserving vital information through two methodologies: image embedding and statistical feature extraction. Additionally, measured temperature information is incorporated. A schematic block diagram of this process is depicted in Fig. 2. Overall, three types of features were used:

- **Image Embedding.** We employed CLIP-ViT-B-3217 (Contrastive Language Image Pre-training Visual Transformer B-32), which encodes images into a vector containing 512 features. The CLIP17 encoding involved mapping images into a high-dimensional embedding space, where each image was represented by a distinctive embedding vector. This was achieved through pre-training a neural network on a vast dataset of image and text pairs using a contrastive loss function. The designation 'B-32' specifies the specific architecture and configuration utilized in this study.
- **Thermal Features.** Temperature data associated with the IRT image dataset, such as minimum, maximum, and ambient temperatures for each image, were manually annotated by observers during image capture and were added to each image. We aimed to assess if this information enhanced interim outcomes and aided in aligning the model between color and temperature.
- **Color Statistical Features.** Five additional statistical features were computed for each color channel of the cropped image, resulting in 15 supplementary features. These statistical features included the mean, standard deviation, coefficient of variance, 90th percentile, and 95th percentile. The final feature vector per image comprises 530 features and is synthesized by concatenating all three sets of features: CLIP, statistical features, and dataset temperature. Image preprocessing typically includes image normalization¹⁹. Therefore, prior to concatenation, all features are individually normalized to reside within the range $[-1, 1]$. Subsequently, Z-score normalization²⁰ is applied to all features together per image, where each feature x is transformed to $\frac{x-\mu}{\sigma}$, with μ representing the mean value of the features and σ representing the standard deviation.

This combined feature vector is then used as input for the classification models (NuSVC for DD Identification and Gaussian Naive Bayes for DD Next-Day Prediction) which we describe next. By fusing these diverse features, the model can leverage both the high-dimensional semantic information from the CLIP embeddings and the more specific color and thermal information, potentially capturing subtle indicators of DD that might not be apparent in any single feature type alone.

Architectures and hyperparameter tuning

For classification, we customized our approach by training models specifically on our dataset. We employed two different architectures:

- **DD Classification.** We used a Nu-Support Vector Classification (NuSVC) model. The NuSVC classifier aims to find the optimal hyperplane that maximizes the margin between classes while allowing for some misclassifications.
- **DD Next-Day Prediction.** We utilized a Gaussian Naive Bayes classifier. This probabilistic model assumes feature independence and calculates the posterior probability using Bayes' theorem. To optimize the performance of our customized DD Identification model we employed a grid search method for hyperparameter tuning. The NuSVC model used in DD Identification, we tuned the following hyperparameters: (i) nu, which controls the number of support vectors and training errors, (ii) kernel, which specifies the kernel type to be used in the algorithm and (iii) gamma, which is kernel coefficient for 'rbf', 'poly' and 'sigmoid' kernels. The grid search was performed using 5-fold cross-validation on a randomly selected training subset of the data to find the best combination of hyperparameters. The Gaussian Naive Bayes classifier model utilized DD Next-Day Prediction was utilized with default parameters: the model assumes equal class priors and smoothing equal to $1e-9$, parameter used to add a small value to the variance of each feature to avoid division by zero.

Full DD classification and prediction pipelines

Figure 3 presents the DD classification pipeline, which uses a Nu-Support Vector Classification (NuSVC) model (with a default threshold of 0.5) as described above.

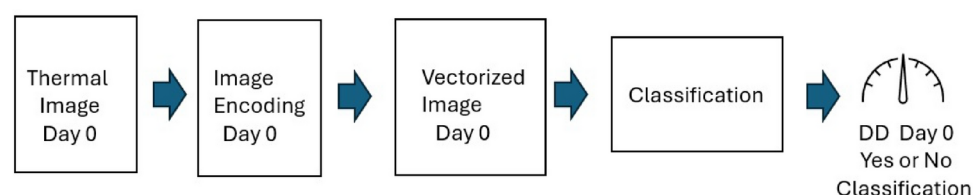


Figure 3. DD Day 0 classification pipeline.

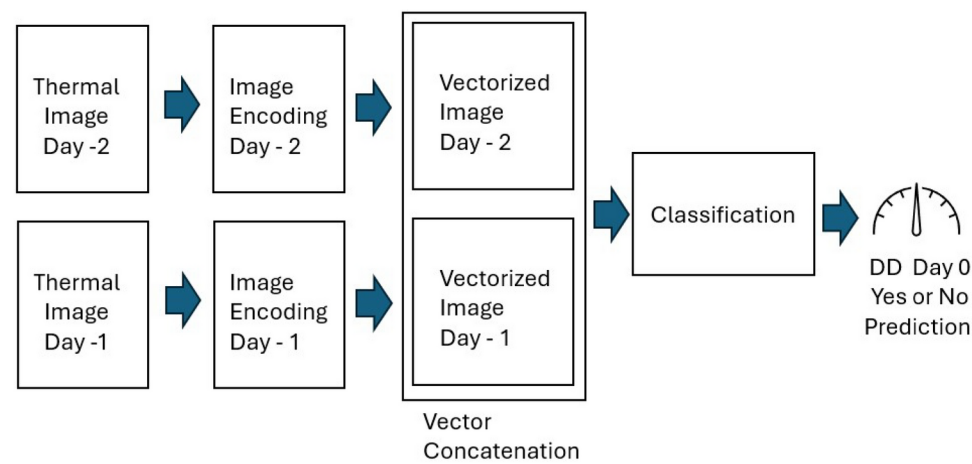


Figure 4. DD early onset prediction pipeline.

Pipeline	Angle	Features	Accuracy	Recall	Precision	F1	Sensitivity	Specificity
Onset Detection	CB	All	0.8115	0.8361	0.7969	0.816	0.8361	0.7869
		Only Embedding	0.8196	0.8361	0.8095	0.8226	0.8361	0.8033
		Only Additional	0.4754	0.4262	0.4727	0.4483	0.4262	0.5246
	Heel	All	0.6667	0.9048	0.6129	0.7308	0.9048	0.4286
		Only Embedding	0.6786	0.9048	0.623	0.7379	0.9048	0.4524
		Only Additional	0.619	0.7619	0.5926	0.6666	0.7619	0.4762
Prediction	CB	All	0.5667	0.5333	0.5714	0.5717	0.5333	0.6
		Only Embedding	0.5667	0.5333	0.5714	0.5717	0.5333	0.6
		Only Additional	0.6667	0.6667	0.6667	0.6667	0.6667	0.6667
	Heel	All	0.55	0.5	0.5556	0.5263	0.5	0.6
		Only Embedding	0.6	0.6	0.6	0.6	0.6	0.6
		Only Additional	0.6	0.5	0.625	0.5556	0.5	0.7

Table 1. Onset detection and prediction classification results.

The predictive pipeline, forecasting a future DD event extends the classification pipeline with several modifications. Rather than evaluating a single image feature vector, we concatenate the feature vectors of images taken from same angle (CB or Heel) of two sequential days: Day -2 and Day -1 (prior to Day 0). To ensure dataset completeness for two days leading up to a day with a healthy cow, we selected days that are as distant from day 0 as possible, such as days -7 and -6 (which may not be present for every cow in the dataset). Two dataset subsets, comprising balanced records of 30 and 20 pairs of feature vectors from CB and Heel angles respectively, served as input for training a new Gaussian Naive Bayes classifier (with a default threshold value of 0.5). Figure 4 presents the resulting pipeline.

Results

Table 1 presents the performance of the machine learning pipeline using accuracy, precision, recall, F1 score, sensitivity, and specificity²¹. For each type of pipeline and angle, three different sets of results were provided: utilizing all described features, leveraging only embedding features, or utilizing only additional features (color statistical features and measured thermal features).

Summary and discussion

Our analysis revealed several key insights regarding the outcomes of the onset detection and prediction pipelines. Evaluation of the Onset Detection Pipeline involved two distinct angles: ‘CB’ (Coronary Band) and ‘Heel’. For the ‘CB’ angle, leveraging all features results in an accuracy and F1 of approximately 0.8115 and 0.816. Focusing solely on embedding features improved the accuracy marginally to about 0.8196 and 0.8226. Conversely, employing only additional features led to markedly lower performance metrics. Similar trends were observed for the ‘Heel’ angle, where utilizing all features yielded an accuracy and F1 of roughly 0.6667 and 0.7308, respectively. Prioritizing embedding features enhanced accuracy and F1 slightly to approximately 0.6786 and 0.7279, while relying solely on additional features resulted in inferior performance, compared to embedding features. Similar to the onset detection pipeline, the prediction pipeline was evaluated from both angles: CB and Heel. When employing all features, the best prediction accuracy and F1 reached approximately 0.6500 and

0.6667, respectively. However, restricting the analysis to embedding features decreased best accuracy and F1 to 0.6330 and 0.6207, and by utilizing only additional features yielded the maximal accuracy and F1 to 0.7000 and 0.7097.

Overall, current findings suggest that prioritizing embedding features significantly enhances the performance of the onset detection pipeline, underlining the importance of image data as the primary source of information. This eliminates the necessity for external registration or additional statistical computations. However, this observation does not extend to the Prediction pipeline. It's worth noting that the performance of the prediction pipeline might be influenced by the limited number of samples in the dataset, potentially impacting the reliability of classification results. Moreover, the prediction accuracy falls behind that of the onset detection, highlighting the challenges in accurately predicting disease occurrences based on thermal images. Additionally, across various performance metrics, the 'CB' angle consistently outperforms the 'Heel' angle in image capture, suggesting it as the preferred angle for optimal results. Our findings are in accordance with those previously reported by¹⁵, regarding the most suited IRT measurement point.

Although significant research efforts were made in the last decades to identify DD susceptibility factors and to mitigate DD effects on animal welfare and production levels, little progress in lowering the prevalence of the disease was made²². A great number of developing DD risk factors were identified, e.g. environmental, genetic and management factors. If validated under commercial systems, our approach could help farmers improve their DD management practices, in order to better diagnose DD and apply more rapid treatments on their farms. Our results are encouraging and of importance, especially when it comes to DD prediction. These results could translate in veterinary care before the first DD clinical signs appear, improving animal wellbeing and reducing the negative effects that a DD episode has on lactation²³ and reproductive²⁴ performance. Furthermore, this approach might also be used to quantify the effectiveness of early applied treatment, throughout tracking recovery and recurrence of cases, as previously suggested by Stokes et al.²⁵.

This study is not without limitations. Firstly, the number of lactating dairy cows that developed DD cases and were found eligible for enrolment in the trial was less than ideal (suboptimal), an increase of the monitored animals is expected to lead to higher performance for both detection and prediction models developed and tested. Therefore, for our future studies we plan to include a higher number of individuals and farms, if possible, with different barn and floor designs, testing thus the models developed under more diverse environments. Furthermore, for the current trial we used a high-sensitivity IRT camera, which would have a significant higher cost associated drawback for on-practice use, potentially representing a risk for on-farm adoption due to economic constraints. To overcome such shortcomings, a number of authors recommend the integrated use of PLF approaches, such as accelerometer data, image analysis systems^{26,27} pressure sensors, radio-frequency identification and ultra-wideband technology, thus in the near future, progress on predicting and automated detection of DD episodes is expected^{28–30}. Previous research in this field outlined that IRT use could represent a cost- and time effective tool, being reliable as well as non-invasive, and showing great potential for remote sensing and automatization in monitoring early indicators for health abnormalities in dairy cattle^{31,32}. To conclude, our applied models achieved performances of above 81% accuracy on DD detection on 'day 0' (first appearance of clinical signs), and above 65% accuracy prediction of DD two days prior to the first appearance of clinical signs. These results are comparable to what was achieved in Magana et al.¹⁴ based on behavioral data collected by accelerometers, for early-onset detection and prediction of DD in cows, reaching 79% and 64% respectively. Therefore, the combination of IRT and sensor-based approaches seems particularly promising for future work developing future real-time automated tools to monitoring DD in commercial dairy farms.

Data availability

Data is available from the corresponding author upon request.

Received: 27 July 2024; Accepted: 22 November 2024

Published online: 02 December 2024

References

- Kulow, M. et al. Evaluation of the prevalence of digital dermatitis and the effects on performance in beef feedlot cattle under organic trace mineral supplementation. *J. Anim. Sci.* **95**, 3435–3444 (2017).
- Orsel, K. et al. Missing pieces of the puzzle to effectively control digital dermatitis. *Transbound. Emerg. Dis.* **65**, 186–198 (2018).
- Vanhoudt, A. et al. Interobserver agreement of digital dermatitis m-scores for photographs of the hind feet of standing dairy cattle. *J. Dairy Sci.* **102**, 5466–5474 (2019).
- Holzhauser, M., Kalsbeek, S. & Frankena, K. Evaluation of selected risk factors for different stages of digital dermatitis in dutch dairy cows. *Vet. J.* **304**, 106086 (2024).
- Dahl-Pedersen, K., Foldager, L., Herskin, M. S., Houe, H. & Thomsen, P. T. Lameness scoring and assessment of fitness for transport in dairy cows: Agreement among and between farmers, veterinarians and livestock drivers. *Res. Vet. Sci.* **119**, 162–166 (2018).
- Van Hertem, T. et al. Lameness detection based on multivariate continuous sensing of milk yield, rumination, and neck activity. *J. Dairy Sci.* **96**, 4286–4298 (2013).
- Arcidiacono, C., Porto, S., Mancino, M. & Cascone, G. Development of a threshold-based classifier for real-time recognition of cow feeding and standing behavioural activities from accelerometer data. *Comput. Electron. Agric.* **134**, 124–134 (2017).
- Taneja, M. et al. Machine learning based fog computing assisted data-driven approach for early lameness detection in dairy cattle. *Comput. Electron. Agric.* **171**, 105286 (2020).
- Neethirajan, S. The role of sensors, big data and machine learning in modern animal farming. *Sens. Bio-Sens. Res.* **29**, 100367 (2020).
- Casella, E., Cantor, M. C., Setser, M. M. W., Silvestri, S. & Costa, J. H. A machine learning and optimization framework for the early diagnosis of bovine respiratory disease. *IEEE Access* (2023).
- Borchers, M., Chang, Y., Tsai, I., Wadsworth, B. & Bewley, J. A validation of technologies monitoring dairy cow feeding, ruminating, and lying behaviors. *J. Dairy Sci.* **99**, 7458–7466 (2016).

12. Pavlenko, A. et al. Influence of digital dermatitis and sole ulcer on dairy cow behaviour and milk production. *Animal* **5**, 1259–1269 (2011).
13. Thomas, A. D., Orsel, K., Cortés, J. A. & Pajor, E. A. Impact of digital dermatitis on feedlot cattle behaviour. *Appl. Anim. Behav. Sci.* **244**, 105468 (2021).
14. Magana, J. et al. Machine learning approaches to predict and detect early-onset of digital dermatitis in dairy cows using sensor data. *Front. Vet. Sci.* **10** (2023).
15. Harris-Bridge, G. et al. The use of infrared thermography for detecting digital dermatitis in dairy cattle: What is the best measure of temperature and foot location to use?. *Vet. J.* **237**, 26–33. <https://doi.org/10.1016/j.tvjl.2018.05.008> (2018).
16. Anagnostopoulos, A. et al. A study on the use of thermal imaging as a diagnostic tool for the detection of digital dermatitis in dairy cattle. *J. Dairy Sci.* [SPACE] <https://doi.org/10.3168/jds.2021-20178> (2021).
17. Cernek, P., Bollig, N., Anklam, K. & Döpfer, D. Hot topic: Detecting digital dermatitis with computer vision. *J. Dairy Sci.* **103**, 9110–9115 (2020).
18. Aravamuthan, S., Walleiser, E. & Döpfer, D. Benchmarking analysis of computer vision algorithms on edge devices for the real-time detection of digital dermatitis in dairy cows. *Prev. Vet. Med.* **231**, 106300 (2024).
19. Pal, K. K. & Sudeep, K. Preprocessing for image classification by convolutional neural networks. In *2016 IEEE International Conference on Recent Trends in Electronics, Information & Communication Technology (RTEICT)*, 1778–1781 (IEEE, 2016).
20. Fei, N., Gao, Y., Lu, Z. & Xiang, T. Z-score normalization, hubness, and few-shot learning. In *2021 IEEE/CVF International Conference on Computer Vision (ICCV)*, 142–151. <https://doi.org/10.1109/ICCV48922.2021.00021> (2021).
21. Feighelstein, M. et al. Automated recognition of pain in cats. *Sci. Rep.* **12**, 9575 (2022).
22. Palmer, M. A. & O'Connell, N. E. Digital dermatitis in dairy cows: A review of risk factors and potential sources of between-animal variation in susceptibility. *Animals* **5**, 512–535 (2015).
23. Relun, A., Lehebel, A., Chesnin, A., Guatteo, R. & Bareille, N. Association between digital dermatitis lesions and test-day milk yield of holstein cows from 41 french dairy farms. *J. Dairy Sci.* **96**, 2190–2200 (2013).
24. Alawneh, J., Laven, R. & Stevenson, M. The effect of lameness on the fertility of dairy cattle in a seasonally breeding pasture-based system. *J. Dairy Sci.* **94**, 5487–5493 (2011).
25. Stokes, J., Leach, K., Main, D. & Whay, H. An investigation into the use of infrared thermography (irt) as a rapid diagnostic tool for digital dermatitis in dairy cattle. *Vet. J.* (2011).
26. Kumar, S., Singh, S. K., Abidi, A. I., Datta, D. & Sangaiah, A. K. Group sparse representation approach for recognition of cattle on muzzle point images. *Int. J. Parallel Prog.* **46**, 812–837 (2018).
27. Kumar, S. & Singh, S. K. Cattle recognition: A new frontier in visual animal biometrics research. *Proc. Natl. Acad. Sci., India, Sect. A* **90**, 689–708 (2020).
28. Ruuska, S., Kajava, S., Mughal, M., Zehner, N. & Mononen, J. Validation of a pressure sensor-based system for measuring eating, rumination and drinking behaviour of dairy cattle. *Appl. Anim. Behav. Sci.* **174**, 19–23 (2016).
29. Achour, B., Belkadi, M., Filali, I., Laghrouche, M. & Lahdir, M. Image analysis for individual identification and feeding behaviour monitoring of dairy cows based on convolutional neural networks (cnn). *Biosys. Eng.* **198**, 31–49 (2020).
30. Ren, K., Bernes, G., Hetta, M. & Karlsson, J. Tracking and analysing social interactions in dairy cattle with real-time locating system and machine learning. *J. Syst. Architect.* **116**, 102139 (2021).
31. Alsaad, M., Schaefer, A. L., Büscher, W. & Steiner, A. The role of infrared thermography as a non-invasive tool for the detection of lameness in cattle. *Sensors* **15**, 14513–14525 (2015).
32. McManus, R. et al. Thermography for disease detection in livestock: A scoping review. *Front. Vet. Sci.* **9**, 965622 (2022).

Acknowledgement

This work was supported by a grant of the Ministry of Research, Innovation and Digitization, CNCS—UEFISCDI, project number PN-III-P1-1.1-TE-2021-0027, within PNCDI III.

Author contributions

A.A.P. conceived the experiment and coordinated the work; J.M. and D.G. collected and analyzed the primary data; M.F., A.M., T.M. and A.Z. analyzed and interpreted the results; M.F., A.M. and T.M. conceptualized the manuscript; A.A.P., G.D. and A.Z. performed final manuscript revision. All authors reviewed the manuscript.

Competing interests

The authors declare no competing interests.

Additional information

Supplementary Information The online version contains supplementary material available at <https://doi.org/10.1038/s41598-024-80902-4>.

Correspondence and requests for materials should be addressed to D.G. or A.Z.

Reprints and permissions information is available at www.nature.com/reprints.

Publisher's note Springer Nature remains neutral with regard to jurisdictional claims in published maps and institutional affiliations.

Open Access This article is licensed under a Creative Commons Attribution-NonCommercial-NoDerivatives 4.0 International License, which permits any non-commercial use, sharing, distribution and reproduction in any medium or format, as long as you give appropriate credit to the original author(s) and the source, provide a link to the Creative Commons licence, and indicate if you modified the licensed material. You do not have permission under this licence to share adapted material derived from this article or parts of it. The images or other third party material in this article are included in the article's Creative Commons licence, unless indicated otherwise in a credit line to the material. If material is not included in the article's Creative Commons licence and your intended use is not permitted by statutory regulation or exceeds the permitted use, you will need to obtain permission directly from the copyright holder. To view a copy of this licence, visit <http://creativecommons.org/licenses/by-nc-nd/4.0/>.

© The Author(s) 2024